JOURNAL OF MECHANICAL ENGINEERING AND SCIENCES (JMES)
ISSN: 2289-4659 e-ISSN: 2231-8380
VOL. 14, ISSUE 3, 6993 – 7016
DOI: https://doi.org/10.15282/jmes.14.3.2020.03.0548

ORIGINAL ARTICLE

Design of a new steerable in-pipe inspection robot and its robust control in presence of pipeline flow

H. Tourajizadeh[1*], A. Sedigh[1], V. Boomeri[1], M. Rezaei[1]

[1] Mechanical Engineering Department, Faculty of Engineering, Kharazmi University, Tehran, Iran

ABSTRACT – Robust multivariable control of an in-pipe inspection robot with variable pitch rate is performed in this paper which moves through the pipelines while fluid is flowing. Most of the traditional inpipe robots have two challenges which make difficulty for investigating the pipe line. The necessity of blocking the flow and difficulty toward bypassing the probable obstacles in the pipes. Here a new mechanism of inpipe robot is proposed which can bypass the obstacles as a result of its mechanism modification and also is able to work in presence of flow by the aid of its designed robust controlled. To meet this goal, the proper mechanism is designed and its related model is derived. Afterwards a nonlinear robust controller is designed and implemented on the proposed robot based on Sliding Mode Control (SMC). The efficiency of the designed robot for bypassing the obstacles and also the robustness of its corresponding controller in presence of flow are investigated by the aid of MATLAB simulation. These simulations are validated by modeling the system in ADAMS and comparing the response of the proposed SMC and Feedback Linearization (FL). It is proved that the designed robot is able to move with controllable velocity through full pipelines while the designed controller can successfully cancel the fluid flow disturbances with a good accuracy of order 10^{-2}.

ARTICLE HISTORY
Revised: 29th Apr 2020
Accepted: 03rd May 2020

KEYWORDS
In-pipe inspection robot; pitch rate controllability; robust control; sliding mode control; pipeline stream

INTRODUCTION

In pipe inspection robots are necessary mobile mechanisms toward verifying the correctness of the pipeline installations and even implementing some manipulating tasks. Variety types of in-pipe robots are proposed so far each of which with different features and capabilities. The main objectives of improvement of the mentioned robots are optimizing their hardware mechanism and increasing the robustness of their software control center. There are two challenges which make difficulty for investigating the pipe lines, using the traditional inpipe robots. The first one is the existence of obstacles at the inner surface of the pipe such as the solid sediments of the fluid which deviates the robot from its desired path. The second one is the necessity of blocking the flow which is impossible for some industries or at least costly. In this paper it is tried to propose a new mechanism which can solve the first challenge, while the second one is covered by designing a robust controller. The first generation of inpipe robot locomotion mechanism was based on wheels. However these robots didn't have any mechanism to ensure the stability of the robot trough different pipe situations. Simba et.al. [1] focused on generating smooth trajectories with using piecewise Bezier curves for a wheeled non-holonomic mobile robot. Also, they considered ideal properties to study the mentioned purpose. Scaglia et.al. [2] investigated the problem of modelling the errors and demonstrated the zero convergence of tracking errors under polynomial un-certainties. Filaretov and Pryanichnikov [3] addressed and investigated the problem of creating an innovative technology for the engineers' study on the basis of the so called "recurrent" method by forming scientific and R&D technical tasks for students as well as their engagement in the administration of software and hardware for mobile robots. Liu and Jiang [4] proposed a new class of distributed nonlinear controllers for leader-following formation control of unicycle robots without global position measurements. They proposed non-linear small-gain methods in order to deal with the problem caused by the non-holonomic constraint of the unicycle robot and yield simple conditions for practical implementation. Moghadam et al. has developed a wheeled based locomotion inpipe robot which is able to pass through the elbows. The robot employs three legs comprised of parallelogram linkages mechanism which enables adapting to various elbow joints in the piping systems [5].

These kinds of robots that are mobile without any mechanism for stabilizing are not useful for pipe-investigations since they suffer from instability especially during tracking curvature paths and they also cannot move through vertical pipes. So, new mobile robots were designed which were adaptable with pipe line conditions and were more practical for in pipe investigations using different locomotion mechanisms. Suzumori et.al [6] designed an in-pipe robot called "snaking drive" that could adapt itself with pipe diameter. But these kinds of robots that have no wheels for smooth motion are too slow and can't provide a fast movement. Thus, proper mechanisms were employed for in-pipe robots i.e. caterpillar and wheel in order to modify their movement. Nagaya er.al. [7] proposed a simple caterpillar robot with a new feature i.e. magnetic in caterpillar that provides the ability of moving through the vertical pipes and also increases the robot's stability. To design a flexible robot Ciszewski et.al. [8] presented a robot with a new mechanism to operate in

*CORRESPONDING AUTHOR | H. Tourajizadeh | ✉ Tourajizadeh@khu.ac.ir

circular and rectangular pipes and ducts oriented horizontally and vertically. Kwon and Yi [9] designed a new caterpillar robot with new property of caterpillar in order to provide a good frictional condition between the pipe's wall and the robot system. It also uses a differential drive to steer the robot and spring loaded four-bar mechanisms to assure the leg's expansion to the pipes' wall. In order to increase the adaptability of the robot with geometrical condition of the pipes Park et.al. [10] proposed a caterpillar robot that can adapt itself with pipe diameter and it has an angular sensor to sense the curvature of the pipes during turning of the robot. In [11] an inchworm in-pipe robot is considered for path planning using GA. The robot is a helical drive in-pipe robot with multiple sub-robots connected together with conic springs just like the wagons of a train in order to move through the curved pipes with a good maneuverability. Caterpillar robots are so useful in slippery pipes since the caterpillar can provide a good friction between the robot and pipe's wall but the mobility of the wheeled robots are better, so some researchers investigated and proposed wheeled based robots with modified mechanisms for increasing their stability. Suzumori et.al. A discussion about the design of the wheeled robots that are omnidirectional and have active stabilizing control is provided by Dertien et.al.[12]. The stability of the mentioned inpipe robot can be increased using screw shaped locomotion mechanism. In [13] path planning of a screw-based in-pipe robot is investigated subject to energy optimization. Here energy consumption is investigated for three different planned path including minimum-energy, sinusoidal, and loss-minimization paths. There is also another type of wheeled robot in which the angular screw motion of a hull section is converted to a straight translational motion. This transfer occurs as a result of inclined angle of the frontal wheels. Since the in-pipes robot should be also capable of passing through the curved pipes, some special designs are proposed to meet the mentioned goal. Kakogawa et.al [14] introduced an in pipe robot equipped by an elastic arms which can move through the bents pipes and pipes with egg-shaped cross section. Another robot which can move through the bents of horizontal or vertical pipes, is studied by Li et.al.[15]. The proposed robot is an in-pipe robot with adaptive linkage. Peng Li et.al [16] designed a novel screw-based in pipe robot which can move through both circular and square tube pipe-lines with curvature using a wall pressed mechanism. Helical drive in-pipe robots are usually designed with passive wheels however, Yonghua Chen et.al [17] proposed a new mechanism of in-pipe robot in which the wheels are synchronized by connecting timing belt. The experimental tests show better traction force for this novel in-pipe robot.

The in-pipe robots can be also equipped by magnets to adhere the steel pipes and move through them. In a work accomplished by Jason Liu et.al. [18] a miniature magnetic in-pipe robot is proposed in which the movement through the small pipes with diameter of 50mm is realized by the aid of some magnets attached to the wheels. To extract the kinematics of screw in-pipe inspection robot, Nayak and Pradhan [19] designed a screw type robot in straight and bent pipes. A new type of telescopic in-pipe robot is designed in this article, which is driven by step motor and screw, and supported by wheels. The robot has advantages of waterproof grade of IP68, stable motion state, and larger traction force. Through force analysis and calculation, its maximum climbing angle is larger than 35°. The robot has good passing ability through the pipelines with bends [20]. Obstacle avoidance is not considered in previous researches. Li et.al [21] proposed a screw robot with one motor that can change its job automatically in order to pass the obstacle. However since it has just one controlling input, its maneuverability is constrained. Yanheng et.al. [22] proposed a flexible steering mechanism in order to move in branches of the pipes. The mentioned researches are limited to designing the robot and no impressive controlling strategy is proposed for them. Following studies focus on design and implementation of a closed loop controller in order to increase the robustness of the robot in front of disturbances and parametric uncertainties. A screw drive in-pipe robot based on adaptive linkage mechanism is proposed in [23] by Li. Et al. The differential property of the adaptive linkage mechanism allows the robot to move without motion interference in the straight and varied curved pipes by adjusting inclining angles of rollers self-adaptively. In order to improve the adaptability to the variable resistance, a torque control method based on the fuzzy controller is proposed. This controller is numeric and needs offline programming which is not suitable for online and real-time applications.Pyrkin and Pitanga et.al. [24] proposed a controller for mobile robots that has "consecutive compensator" and "MPC". Although the robustness of the mentioned robot is increased, but it cannot be controlled in the presence of the fluid stream. A screw robot was investigated by Heidari et.al. [25] in live water stream and they extracted the kinematics and dynamics of the system while fuzzy-logic controller is employed for stabilizing the system which is numeric and is not preferable.

As can be seen in the literature, a robust analytic controller is ignored for in pipe robots which are steerable. Considering the fact that the robustness of the Sliding Mode Controller (SMC) is significantly high, implementing of this controller for multi input in pipe robots which are usually exposed to flowing fluid can be extremely useful. SMC has been implemented for some similar mechanisms so far; Sliding mode is a strong nonlinear robust controller which can be employed for the vast variety of robots. Adaptive sliding mode control is implemented for a novel cable driven robot to increase the end-effector performance in presence of disturbances [26]. In [27] a robust controller based on back stepping method and sliding mode control method is designed for a wheeled omnidirectional mobile robots. Here the sliding mode control compensates the parametric uncertainties and external disturbances for a 4-wheels omnidirectional robot. There are also some studies proposing new controlling ideas which are robust and can compensate the disturbancers, but they are have been employed for simple plants such as motors or elastomers so far [28, 29].Most researches in the field of in pipe robots are limited to moving through the empty pipes while in many cases blocking the flow of the fluid is not possible or even cost full. There are few researches in which the screw in pipe robots is considered in presence of water flow however no robust controller is proposed in these papers [30].

To sum up, investigating the mentioned literatures shows that first of all, the previous screw robots have fixed wheels angle which are not steerable. Thus it is not possible to by-pass the probable obstacles. Secondly most of them are considered in the pipes with no flowing fluid which ignores the effect of real disturbances. Thus it is necessary to block

the stream of the pipe. And finally a robust analytic multivariable controller is not implemented on this kind of robots so far, to control them in presence of obstacles and drag forces. The goal of this paper is to design a robust analytic controller for the mentioned steerable in-pipe robot with two controlling input to increase its stability and robustness in presence of pipeline flow. This robot is able to bypass the obstacles and move through the live pipe with flowing fluid. To cover the mentioned goal, first of all, the mechanism is improved to increase its maneuverability in presence of obstacles. Kinematics and kinetics of the proposed variable pitch rate screw robot is represented. Afterwards, considering the multi input-multi output (MIMO) structure of the corresponding state space, the design procedure of a proper controller based on robust approach of SMC is presented in presence of external disturbance of fluid drag forces. In the next section the superiority of the designed robot and the efficiency of the implemented controller is verified by the aid of a series of analytic simulations performed in the MATLAB and SIMULINK. The proposed robot is also modeled in ADAMS and it is exported to the SIMULIMK in order to compare the efficiency of the proposed controller in presence of drag forces relative to conventional FL method. It is shown that, not only the possibility of controlling the pitch rate of the robot movement is provided by the aid of the proposed mechanism, but also its robust control is guaranteed in presence of external disturbances of flowing fluid using the SMC approach.

KINEMATICS AND DYNAMICS

Kinematics

The robot consists of a stator with three fixed angle wheels and a rotor with three angled wheels as shown in Figure 1. The locomotion of the robot is realized by screw shaped rotation of the rotor part of the robot within the pipe by the aid of its installed angled wheels. Traditional versions of this robot had a fixed angle for the angled wheels which caused a fixed pitch rate for the robot movement. The new proposed screw in-pipe robot in this paper has steerable angled wheels which result in controllable pitch rate for the robot movement.

Therefore, previous models of this kind robots had just one input and two states. But in this paper the system is considered steerable and so, one degree of freedom and one input is added to the system which eventually causes increasing the states of the system from 2 to 4.

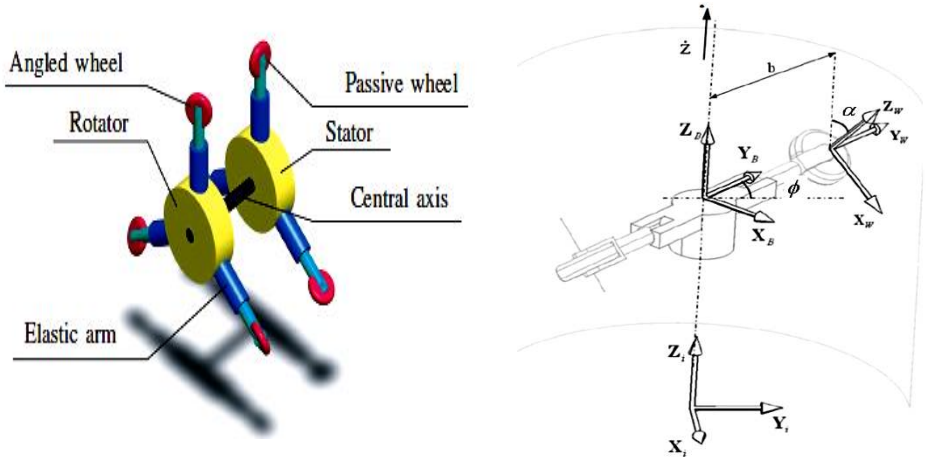

(a) (b)

Figure 1. (a) A screw in-pipe inspection robot [31] and (b) The parameters on one pair of wheels without passive wheels

To meet this goal, a differential based gearbox system is added to the steering mechanism, according to the Figure 2 which controls the angle of all of the three front legs simultaneously by a unique motor. This differential is prepared using four interconnected bevel gears. The driver gear is connected to the input controlling motor while the driven gears are connected to the wheels.

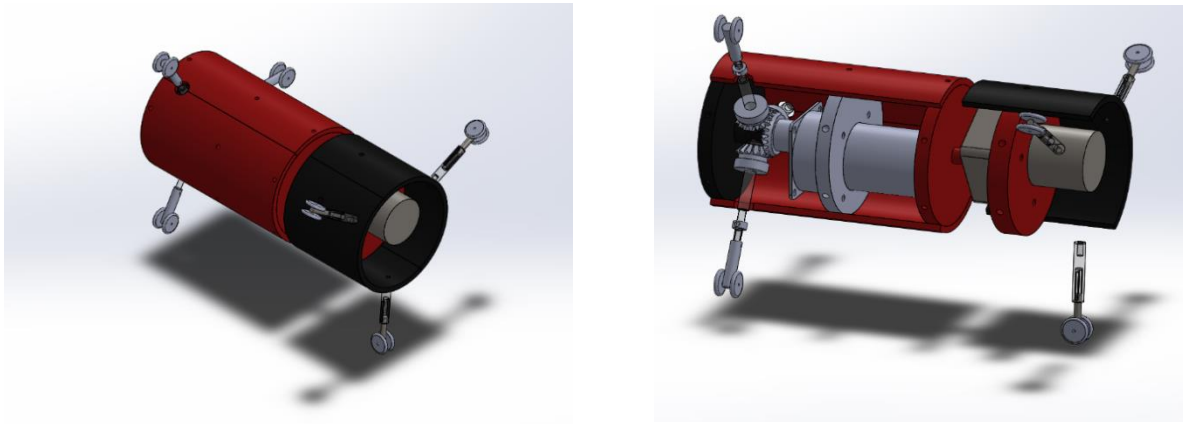

(a) (b)

Figure 2. (a) Proposed steerable screw inpipe robot and (b) The scheme of the added differential gear for the steer module

Thus, the new Jacobian matric needs to be extracted. In this paper the states are $(\emptyset.\dot{\emptyset}.\alpha \; and \; \dot{\alpha})$ in which $\emptyset$ is the angle of the hull and α is the angle of the wheels. For infinitesimal motion along z direction which is the pipe line direction, there are two equations that demonstrate the kinematic relation between the robot rotation θ with $\emptyset$ and α and the relation between z distance with $\emptyset$, α.

$$dz = (b+r)d\phi\tan(\alpha) \tag{1}$$

$$d\theta = \left(\frac{b+r}{r\cos(\alpha)}\right)d\phi \qquad \alpha \neq \frac{\pi}{2} \tag{2}$$

As shown in Figure 1(b), b is the distance between the center of the robot and the center of the wheel, r is the radius of the wheels and we have$R = (r + b)$ which is the radius of the pipe. The translation matric of the system which translates the local center of the robot to its related global position, will be as Tz.

$$T_z = \begin{bmatrix} 1 & 0 & 0 & 0 \\ 0 & 1 & 0 & 0 \\ 0 & 0 & 1 & R\phi\tan(\alpha) \\ 0 & 0 & 0 & 1 \end{bmatrix} \tag{3}$$

So if at the initial condition the vector of the center of the robot is $p=[0,0,0]$, the position of the robot as a function of $\emptyset$ and α is:

$$H_s = T_z\begin{bmatrix} p \\ 1 \end{bmatrix} = \begin{bmatrix} 0 \\ 0 \\ R\phi\tan(\alpha) \\ 1 \end{bmatrix} \tag{4}$$

Also in order to stablish the relation between the joint space and work space of the robot when $\dot{x}$, $\dot{y}$,$\dot{z}$ are considered as the work space of the robot and $\dot{\alpha}$ and $\dot{\emptyset}$ are considered as the joint space of the robot, the Jacobian matric can be defined as:

$$\begin{Bmatrix} \dot{x} \\ \dot{y} \\ \dot{z} \\ \dot{\phi} \end{Bmatrix} = \begin{bmatrix} 0 & 0 \\ 0 & 0 \\ 0 & R\tan(\alpha) \\ 0 & 1 \end{bmatrix} \begin{Bmatrix} \dot{\alpha} \\ \dot{\phi} \end{Bmatrix} \tag{5}$$

Dynamics

The proposed system can be described with two coupled differential equations relevant to generalized coordinates (α *and* $\emptyset$). The equations of the system are extracted using Lagrangian approach. First of all, it is needed to make L as Eq. (6):

$$L = T - V \tag{6}$$

where T and V denote the kinetic energy and potential energy due to gravitational forces, respectively. Thus the total kinetic energy will be:

$$T = T_{motor} + T_{Hull} + \Gamma(T_{w1} + T_{w2}) \tag{7}$$

where T_{motor}, T_{Hull}, T_{w1} and T_{w2} show kinetic energy of the motor, hull, wheels around the pipe axis and wheels around the legs, respectively. Γ denotes the number of steering wheels. In Eq. (7) the kinetic energy of the passive straight wheels is ignored. Therefore, total kinetic energy of the system can be described as:

$$T = \frac{1}{2}\left\{\left((b+r)\frac{S_\alpha}{C_\alpha}\right)^2 \alpha_M + \Gamma b^2 \alpha_m + I_B\right\}\dot{\phi}^2 + \frac{1}{2}\Gamma I_{weel}\dot{\alpha}^2 \tag{8}$$

where S and C denotes the *Sin* and *Cos* of the related angles and:

$$\begin{aligned} \alpha_M &= (M_m + M_h + \Gamma m + \Gamma\frac{I_{WX}}{r^2}) \\ \alpha_m &= (m + \frac{I_{WZ}}{r^2}) \end{aligned} \tag{9}$$

Also I_B and I_{wheel} are moment of inertia of the hull and moment of inertia of the wheel. Moreover M_m and M_h are the mass of the motor and hull respectively, and I_{WX} and I_{WZ} are the wheel moment of inertia about the X and Z axis. An infinitesimal change in the potential energy of the robot due to gravity during the motion along the vertical pipes can be calculated as:

$$dV = (M_m + M_h + \Gamma m)(b+r)g d\phi \tan(\alpha) \tag{10}$$

g is gravitational acceleration and m is the mass of the wheels. As mentioned above, $\emptyset$ *and* α i.e. the angle of rotation of the hull and the variation of the wheels' angle, respectively are considered as the generalized coordinates of the system and so the corresponding Lagrangian equation can be written as:

$$\frac{d}{dt}\left(\frac{\partial L}{\partial \dot{\phi}_i}\right) - \frac{\partial L}{\partial \phi_i} = Q_i \tag{11}$$

where Q_i are the generalized forces which can be identified as Eq. (12) for the present work:

$$\begin{aligned} Q_1 &= T_m - T_f \\ Q_2 &= T_s \end{aligned} \tag{12}$$

In Eq. (12), T_m is the torque generated by the motor relevant to the hull, T_f is the resisting torque due to the friction between the wheels and their axles and T_s is the torque generated by the motor corresponding to the steering wheels.

The friction is one of the most important parameters in the system which guaranties the robot stability, so T_f should be calculated accurately by the aid of Eq. (13):

$$T_f = \Gamma b \mu F_N \sin(\alpha) \tag{13}$$

where, μ is the coefficient of friction and F_N is the normal force exerted on the wheels from the pipe wall. Thus by calculating Eq. (11) the dynamic differential equation of the system in presence of external drag force of the stream can be extracted as:

$$\ddot{\phi} = \frac{\lambda R g(1+\tan^2(\alpha))\dot{\alpha} - 2R^2\alpha_M\frac{S_\alpha}{C_\alpha^3}\dot{\alpha}\dot{\phi} - \Gamma\mu b F_N S_\alpha - K_f x_2 - \frac{AC_D b\rho\sin(x_3)(Rx_2\sin(x_3)+v)^2}{2}}{\Gamma\alpha_m b^2 + I_B + R^2\alpha_M\tan^2(\alpha)} + \frac{T_m}{\Gamma\alpha_m b^2 + I_B + R^2\alpha_M\tan^2(\alpha)} \tag{14}$$

$$\ddot{\alpha} = \left(\frac{R^2\alpha_M\left(\tan(\alpha)+\tan^3(\alpha)\right)}{\Gamma I_{wheels}}\right)\dot{\phi}^2 - \left(\frac{\lambda R g(1+\tan^2(\alpha))}{\Gamma I_{wheels}}\right)\phi + \frac{T_s}{\Gamma I_{wheels}} \tag{15}$$

where λ is the summation of all masses, A is the cross section aria of the robot against the fluid stream, C_D is drag coefficient, ρ is the density of the fluid and v is the relative velocity of the robot with respect to the fluid. Because of steerability of the wheels and increasing the DOFs of the system, the number of differential equations of the system increases to two. In order to solve the mentioned equations, extracting the time responses of the DOFs and finally

controlling the system, it is required to rewrite the equations in the form of state space. Considering $(\emptyset.\dot{\emptyset}.\alpha.\dot{\alpha})$ as the states of the proposed inpipe robot, corresponding state space can be extracted as:

$$\begin{aligned}
\dot{x}_1 &= x_2 \\
\dot{x}_2 &= \frac{\lambda Rg(1+\tan^2(x_3))x_4 - 2R^2\alpha_M S_{x_3} x_4 x_2 - \Gamma\mu b F_N S_{x_3} - K_f x_2 - \frac{AC_D b\rho \sin(x_3)(Rx_2\sin(x_3)+v)^2}{2}}{\Gamma\alpha_m b^2 + I_B + R^2\alpha_M \tan^2(x_3)} \\
&+ \frac{T_m}{\Gamma\alpha_m b^2 + I_B + R^2\alpha_M \tan^2(x_3)} \\
\dot{x}_3 &= x_4 \\
\dot{x}_4 &= \left(\frac{R^2\alpha_M\left(\tan(x_3)+\tan^3(x_3)\right)}{\Gamma I_{wheels}}\right)x_2^2 - \left(\frac{\lambda Rg(1+\tan^2(x_3))}{\Gamma I_{wheels}}\right)x_2 + \frac{T_s}{\Gamma I_{wheels}}
\end{aligned} \tag{16}$$

CONTROL DESIGN

Two nonlinear controlling strategies of feedback linearization and sliding mode are employed here to control the designed robot and the performance of them are compared. It will be shown that in presence of stream drag force as the external disturbances, the former fails while the latter can handle the robot movement in presence of the mentioned disturbance.

Also it should be considered that both of the considered nonlinear controllers of FL and SMC results in stable closed loop system according to Lyapunov theory and their stability are proved .Moreover about the latter case, the robustness of the system can be also guaranteed as the result of defining the related sliding surface.

Feedback Linearization

Considering the fact that the drag force of the flowing fluid is an external disturbance for the robot, sliding mode control approach is employed in order to control and stabilize the system. To meet this goal, exact linearization needs to be implemented on the state space of the system. The following MIMO system is the exact nonlinear presentation of the state space of the present robot:

$$\dot{X} = f(x) + g(x)u + d(t) = \begin{Bmatrix} x_2 \\ \frac{\lambda Rg(1+\tan^2(x_3))x_4 - 2R^2\alpha_M S_{x_3} x_4 x_2 - \Gamma\mu b F_N S_{x_3} - K_f x_2 - \frac{AC_D b\rho \sin(x_3)(Rx_2\sin(x_3)+v)^2}{2}}{\Gamma\alpha_m b^2 + I_B + R^2\alpha_M \tan^2(x_3)} \\ x_4 \\ \left(\frac{R^2\alpha_M\left(\tan(x_3)+\tan^3(x_3)\right)}{\Gamma I_{wheels}}\right)x_2^2 - \left(\frac{\lambda Rg(1+\tan^2(x_3))}{\Gamma I_{wheels}}\right)x_2 \end{Bmatrix} + \begin{bmatrix} 0 & 0 \\ \frac{1}{\Gamma\alpha_m b^2 + I_B + R^2\alpha_M \tan^2(x_3)} & 0 \\ 0 & 0 \\ 0 & \frac{1}{\Gamma I_{wheels}} \end{bmatrix} \begin{bmatrix} T_m \\ T_s \end{bmatrix} + \begin{bmatrix} d(t) \\ 0 \end{bmatrix} \tag{17}$$

$$y = h(x) = \begin{bmatrix} x_1 \\ x_3 \end{bmatrix} \tag{18}$$

where x ($\in \Re^n$) is the state vector, u ($\in \Re^m$) represents controlling inputs of the system, y ($\in \Re^m$) stands for outputs, f and g are nonlinear smooth vector fields, h is a nonlinear smooth scalar function and $d(t)$ is a bounded external disturbance with definite bound of D, that is $|d(t)| \leq D < \infty$.Also Tm and Ts are the controlling input of the system which are the torque of the main body and the angle wheels.

In this section the input-output linearization of the above MIMO system is performed by differentiating the output y of the system till the inputs appear explicitly. So, by differentiating Eq. (18):

$$\dot{y} = L_f h_i + \sum_{j=1}^{m} (L_{gj} h_i) u_j, \qquad i = 1,....,m \tag{19}$$

u is the input of the system and $L_f h$ and $L_g h$ represent the Lie derivatives of $h(x)$ with respect to $f(x)$ and $g(x)$, respectively. For the proposed system, the Eq. (19) is:

$$\begin{bmatrix} \dot{y}_1 \\ \dot{y}_2 \end{bmatrix} = L_f \begin{bmatrix} x_1 \\ x_3 \end{bmatrix} + \sum_{j=1}^{m} (L_{gj} \begin{bmatrix} x_1 \\ x_3 \end{bmatrix}) \begin{bmatrix} T_m \\ T_s \end{bmatrix} \qquad i = 1,2 \tag{20}$$

The key point is that, if $L_{gj} L_f^{(r_i-1)} h_i(x) = 0$ for all j, then the inputs do not appear in Eq. (20), so for $r_1=1$ and $r_2=1$, the Eq. (20) is:

$$\begin{bmatrix} \dot{y}_1 \\ \dot{y}_2 \end{bmatrix} = \begin{bmatrix} x_2 \\ x_4 \end{bmatrix} + \begin{bmatrix} 0 \\ 0 \end{bmatrix} \tag{21}$$

Thus, further differentiation needs to be repeated as:

$$y_i^{(r_i)} = L_f^{(r_i)} h_i + \sum_{j=1}^{m} (L_{gj} L_f^{(r_i-1)} h_i) u_j, \qquad i = 1, ..., m \tag{22}$$

Such that $L_{gj} L_f^{(r_i-1)} h_i(x) \neq 0$ for at least one j. this procedure is repeated for each output y_i. Thus, there will be a set of m equation given by:

$$\begin{bmatrix} y^{(r_1)} \\ y^{(r_m)} \end{bmatrix} = \begin{bmatrix} L_f^{r_1} h_1(x) \\ L_f^{r_m} h_m(x) \end{bmatrix} + j(x) \begin{bmatrix} u_1 \\ u_m \end{bmatrix} \tag{23}$$

So for $r_1=2$ and $r_2=2$, Eq. (23) is as bellow for the proposed robot:

$$\begin{bmatrix} \ddot{y}_1 \\ \ddot{y}_2 \end{bmatrix} = \begin{bmatrix} \dfrac{\lambda R g (1+\tan^2(x_3)) x_4 - 2R^2 \alpha_M S_{x_3} x_4 x_2 - \Gamma \mu b F_N S_{x_3} - K_f x_2 - \dfrac{A C_D b \rho \sin(x_3)(R x_2 \sin(x_3) + v)^2}{2}}{\Gamma \alpha_m b^2 + I_B + R^2 \alpha_M \tan^2(x_3)} \\ \left(\dfrac{R^2 \alpha_M \left(\tan(x_3) + \tan^3(x_3) \right)}{\Gamma I_{wheels}} \right) x_2^2 - \left(\dfrac{\lambda R g (1+\tan^2(x_3))}{\Gamma I_{wheels}} \right) x_2 \end{bmatrix} + j(x) \begin{bmatrix} T_m \\ T_s \end{bmatrix} \tag{24}$$

where $j(x)$ can be expressed as follow:

$$j(x) = \begin{bmatrix} L_{g1} L_f^{r_1-1} h_1 & \cdots & \cdots & L_{gm} L_f^{r_1-1} h_1 \\ \cdots & \cdots & \cdots & \\ \cdots & \cdots & \cdots & \\ L_{g1} L_f^{r_m-1} h_m & & & L_{gm} L_f^{r_m-1} h_m \end{bmatrix} = \begin{bmatrix} \dfrac{1}{\Gamma \alpha_m b^2 + I_B + R^2 \alpha_M \tan^2(x_3)} & 0 \\ 0 & \dfrac{1}{\Gamma I_{wheels}} \end{bmatrix} \tag{25}$$

$j(x)$ is the decoupling matrix for the MIMO systems. If $j(x)$ is nonsingular, then the control law u can be shown as:

$$u = -j^{-1}(x) \begin{bmatrix} L_f^{r_1} h_1(x) \\ \cdots \\ \cdots \\ L_f^{r_m} h_m(x) \end{bmatrix} + g^{-1}(x) \begin{bmatrix} v_1 \\ . \\ . \\ v_m \end{bmatrix} \tag{26}$$

For which can be substituted as bellow for the present system:

$$u = -j^{-1}(x)\left(-\begin{bmatrix} L_f^{r_1}h_1(x) \\ \cdots \\ \cdots \\ L_f^{r_m}h_m(x) \end{bmatrix} + \begin{bmatrix} v_1 \\ \cdot \\ \cdot \\ v_m \end{bmatrix}\right) =$$

$$\begin{bmatrix} \dfrac{1}{\Gamma\alpha_m b^2 + I_B + R^2\alpha_M \tan^2(x_3)} & 0 \\ 0 & \dfrac{1}{\Gamma I_{wheels}} \end{bmatrix}^{-1} \tag{27}$$

$$\left(\begin{bmatrix} \dfrac{\lambda Rg(1+\tan^2(x_3))x_4 - 2R^2\alpha_M S_{x_3}x_4x_2 - \Gamma\mu bF_N S_{x_3} - K_f x_2 - \dfrac{AC_D b\rho\sin(x_3)(Rx_2\sin(x_3)+v)^2}{2}}{\Gamma\alpha_m b^2 + I_B + R^2\alpha_M \tan^2(x_3)} \\ \left(\dfrac{R^2\alpha_M\left(\tan(x_3)+\tan^3(x_3)\right)}{\Gamma I_{wheels}}\right)x_2^2 - \left(\dfrac{\lambda Rg(1+\tan^2(x_3))}{\Gamma I_{wheels}}\right)x_2 \end{bmatrix} + \begin{bmatrix} v_1 \\ \cdot \\ \cdot \\ v_m \end{bmatrix}\right)$$

where $\bar{v} = [v_1 \ldots v_m]$T is the new set of inputs to be defined by the designer.

Normal Form and Internal Dynamics Analysis

The order of the system "*r*" has a significant role in feedback linearization control approach. Indeed, according to the value of this parameter, three following cases can be considered.

Case 1: If $r = n$, then the nonlinear system in Eq. (17) is fully feedback linearizable.

Case 2: If $r < n$, then the nonlinear system in Eq. (17) is partially feedback linearizable. In this case, there are some internal dynamics of order (n-r). In tracking control, it should be guaranteed that these dynamics are not singular, i.e. unstable or unbounded.

Case 3: If r does not exist on the domain D, then the input-output linearization approach is not suitable for the studied case.

As shown in Eq. (24), $r1 = r2 = n = 2$, so the proposed non-linear system of the robot is fully feedback linearizable. In other words, the input-output linearization is exactly the same as input-state linearization.

Sliding Mode Control Design

In this section sliding mode controller is designed for the new in-pipe inspection robot. Consider the MIMO system of Eq. (17). The goal of control design is to propose a control law to decrease the error between the state vector and the desired reference state trajectory $\bar{x}_d = \left(x_d, \dot{x}_d, \ldots, x_d^{(n-1)}\right)$ in the presence of model uncertainties and external disturbances. As there are two coupled second order differential equations here, the errors are:

$$\bar{e}_1 = \bar{x}_1 - \bar{x}_{1d} = \left[e, \dot{e}, \ldots, e^{(n-1)}\right]^{\mathrm{T}} = \left[(x_1 - x_{1d}), \quad (\dot{x}_1 - \dot{x}_{1d})\right]^T \tag{28}$$

$$\bar{e}_2 = \bar{x}_3 - \bar{x}_{3d} = \left[e, \dot{e}, \ldots, e^{(n-1)}\right]^{\mathrm{T}} = \left[(x_3 - x_{3d}), \quad (\dot{x}_3 - \dot{x}_{3d})\right]^T \tag{29}$$

Index d denotes the desired value of the states. Then the sliding surface based on the error state space can be defined by the following equation, so there are two sliding surfaces as follow:

$$s_1 = c_1(x_1 - x_{1d}) + c_2(\dot{x}_1 - \dot{x}_{1d}) \tag{30}$$

$$s_2 = c_1'(x_2 - x_{2d}) + c_2'(\dot{x}_2 - \dot{x}_{2d}) \tag{31}$$

where c, c' are the surface coefficients. In order to guarantee the stability of the designed controller, Lyapunov theory is implemented. The related Lyapunov function is defined according to the sliding surface as follow, and the controlling gains of the sliding mode is determined in a way that results in negative definite function for the Lyapunov derivation. A sufficient condition to ensure the convergence of the error vector $\bar{e}$ to the sliding surface and satisfy the mentioned stability control is to define the control law in the following way:

$$\frac{1}{2}\frac{d}{dt}\left(s^2\right) \le -\eta|s|, \quad \eta > 0 \quad \Rightarrow \quad \frac{1}{2}\frac{d}{dt}\left(\begin{bmatrix} s_1^2 \\ s_2^2 \end{bmatrix}\right) \le -\begin{bmatrix} \eta_1 & 0 \\ 0 & \eta_2 \end{bmatrix}\begin{vmatrix} s_1 \\ s_2 \end{vmatrix}, \begin{bmatrix} \eta_1 & 0 \\ 0 & \eta_2 \end{bmatrix} > 0 \tag{32}$$

where the coefficient η is a positive constant. By simplifying, the sliding condition in Eq. (32) can be rewritten as:

$$s\dot{s} \le -\eta s\,\mathrm{sgn}(s) \;\Rightarrow \begin{bmatrix} s_1 \\ s_2 \end{bmatrix}^T \begin{bmatrix} \dot{s}_1 \\ \dot{s}_2 \end{bmatrix} \le \begin{bmatrix} \eta_1 & 0 \\ 0 & \eta_2 \end{bmatrix} \begin{bmatrix} s_1 \\ s_2 \end{bmatrix}^T \begin{bmatrix} \mathrm{sgn}(s_1) \\ \mathrm{sgn}(s_2) \end{bmatrix} \tag{33}$$

By taking the time derivative of Eqs. (30,31), we obtain:

$$\dot{s} = \sum_{i=1}^{n-1} c_i e^{(i)} + x^{(n)} - x_d^{(n)} = \sum_{i=1}^{n-1} c_i e^{(i)} + f(\bar{x},t) + g(\bar{x},t)u(t) + d(t) - x_d^{(n)} \tag{34}$$

where d is a disturbance with a definite bounded range. so we have:

$$\dot{s}_1 = c_1 \dot{e}_1 + \frac{\lambda Rg(1+\tan^2(x_3))x_4 - \dfrac{2R^2\alpha_M S_{x_3} x_4 x_2}{\cos^3(x_3)} - \Gamma\mu b F_N S_{x_3} - K_f x_2 - \dfrac{AC_D b\rho \sin(x_3)(Rx_2\sin(x_3)+v)^2}{2}}{\Gamma\alpha_m b^2 + I_B + R^2\alpha_M \tan^2(x_3)} + \frac{T_m}{\Gamma\alpha_m b^2 + I_B + R^2\alpha_M \tan^2(x_3)} + d(t) - \ddot{x}_1 \tag{35}$$

$$\dot{s}_2 = c_1' \dot{e}_2 + \left(\frac{R^2\alpha_M \left(\tan(x_3) + \tan^3(x_3)\right)}{\Gamma I_{wheels}} \right) x_2^2 - \left(\frac{\lambda Rg(1+\tan^2(x_3))}{\Gamma I_{wheels}} \right) x_2 + \frac{T_s}{\Gamma I_{wheels}} - \ddot{x}_3 \tag{36}$$

Substituting Eq. (33) into Eqs. (35, 36), sliding condition can be defined as:

$$s_1 \left[c_1 \dot{e}_1 + \frac{\lambda Rg(1+\tan^2(x_3))x_4 - \dfrac{2R^2\alpha_M S_{x_3} x_4 x_2}{\cos^3(x_3)} - \Gamma\mu b F_N S_{x_3} - K_f x_2 - \dfrac{AC_D b\rho \sin(x_3)(Rx_2\sin(x_3)+v)^2}{2}}{\Gamma\alpha_m b^2 + I_B + R^2\alpha_M \tan^2(x_3)} + \frac{T_m}{\Gamma\alpha_m b^2 + I_B + R^2\alpha_M \tan^2(x_3)} + d(t) - \ddot{x}_1 \right] \le \eta_1 s_1 \,\mathrm{sgn}(s_1) \tag{37}$$

$$s_2 \left[c_1' \dot{e}_2 + \left(\frac{R^2\alpha_M \left(\tan(x_3) + \tan^3(x_3)\right)}{\Gamma I_{wheels}} \right) x_2^2 - \left(\frac{\lambda Rg(1+\tan^2(x_3))}{\Gamma I_{wheels}} \right) x_2 + \frac{T_s}{\Gamma I_{wheels}} - \ddot{x}_3 \right] \le \eta_2 s_2 \,\mathrm{sgn}(s_2) \tag{38}$$

By knowing $f(\bar{x}.t)$, $g(\bar{x}.t)$, $d(t)$, the following controlling law based on sliding mode method can be designed in a way that the sliding condition in Eqs. (30, 31) could be guaranteed:

$$\begin{aligned} &if \quad s \ge 0 \rightarrow u^* \le -\frac{1}{g(\bar{x},t)} \left[\sum_{i=1}^{n-1} c_i e^{(i)} + f(\bar{x},t) + d(t) - x_d^{(n)} + \eta\,\mathrm{sgn}(s) \right] \\ &f \quad s < 0 \rightarrow u^* > -\frac{1}{g(\bar{x},t)} \left[\sum_{i=1}^{n-1} c_i e^{(i)} + f(\bar{x},t) + d(t) - x_d^{(n)} + \eta\,\mathrm{sgn}(s) \right] \end{aligned} \tag{39}$$

Therefore if we define $\eta_\Delta \ge \eta \ge 0$ the following controlling input always satisfies the above conditions:

$$u^* = -\frac{1}{g(\bar{x},t)} \left[\sum_{i=1}^{n-1} c_i e^{(i)} + f(\bar{x},t) + d(t) - x_d^{(n)} + \eta_\Delta\,\mathrm{sgn}(s) \right] \tag{40}$$

Based on Eq. (34) and substituting it in Eq. (40), control law for the new proposed system can be presented in matrix form:

$$\begin{bmatrix} u_1^* \\ u_2^* \end{bmatrix} = -\begin{bmatrix} \frac{1}{\Gamma\alpha_m b^2 + I_B + R^2\alpha_M \tan^2(x_3)} & 0 \\ 0 & \frac{1}{\Gamma I_{wheels}} \end{bmatrix}^{-1} \left(\begin{bmatrix} c_1 \dot{e}_1 \\ c_1' \dot{e}_2 \end{bmatrix} + \begin{bmatrix} \frac{\lambda Rg(1+\tan^2(x_3))x_4 - \frac{2R^2\alpha_M S_{x_3} x_4 x_2}{\cos^3(x_3)} - \Gamma\mu b F_N S_{x_3} - K_f x_2 - \frac{AC_D b\rho \sin(x_3)(Rx_2\sin(x_3)+v)^2}{2}}{\Gamma\alpha_m b^2 + I_B + R^2\alpha_M \tan^2(x_3)} \\ \left(\frac{R^2\alpha_M\left(\tan(x_3)+\tan^3(x_3)\right)}{\Gamma I_{wheels}}\right)x_2^2 - \left(\frac{\lambda Rg(1+\tan^2(x_3))}{\Gamma I_{wheels}}\right)x_2 \end{bmatrix} + d(t) - \begin{bmatrix} \ddot{x}_1 \\ \ddot{x}_3 \end{bmatrix} + \begin{bmatrix} \eta_{1\Delta}\,\mathrm{sgn}(s_1) \\ \eta_{2\Delta}\,\mathrm{sgn}(s_2) \end{bmatrix} \right) \tag{41}$$

The control law in Eq. (40) is usually expressed as the summation of two separated laws which are called equivalent and switching controlling terms:

$$u^* = u_{eq} - u_{sw} \tag{42}$$

$$u_{eq} = -\frac{1}{g(\bar{x},t)}\left[\sum_{i=1}^{n-1} c_i e^{(i)} + f(\bar{x},t) + d(t) - x_d^{(n)}\right] \tag{43}$$

$$u_{sw} = \frac{1}{g(\bar{x},t)}\eta_\Delta\,\mathrm{sgn}(s) \tag{44}$$

So for the considered in-pipe inspection robot of this paper the equivalent and switching control laws are as Eqs. (45,46). Thus not only the convergence in sliding surface will be meet but also the stability condition of Lyapunov will be satisfied employing the above controlling effort.

$$\begin{bmatrix} u_{1eq}^* \\ u_{2eq}^* \end{bmatrix} = -\begin{bmatrix} \frac{1}{\Gamma\alpha_m b^2 + I_B + R^2\alpha_M \tan^2(x_3)} & 0 \\ 0 & \frac{1}{\Gamma I_{wheels}} \end{bmatrix}^{-1} \left(\begin{bmatrix} c_1 \dot{e}_1 \\ c_1' \dot{e}_2 \end{bmatrix} + \begin{bmatrix} \frac{\lambda Rg(1+\tan^2(x_3))x_4 - \frac{2R^2\alpha_M S_{x_3} x_4 x_2}{\cos^3(x_3)} - \Gamma\mu b F_N S_{x_3} - K_f x_2 - \frac{AC_D b\rho \sin(x_3)(Rx_2\sin(x_3)+v)^2}{2}}{\Gamma\alpha_m b^2 + I_B + R^2\alpha_M \tan^2(x_3)} \\ \left(\frac{R^2\alpha_M\left(\tan(x_3)+\tan^3(x_3)\right)}{\Gamma I_{wheels}}\right)x_2^2 - \left(\frac{\lambda Rg(1+\tan^2(x_3))}{\Gamma I_{wheels}}\right)x_2 \end{bmatrix} + d(t) - \begin{bmatrix} \ddot{x}_1 \\ \ddot{x}_3 \end{bmatrix} \right) \tag{45}$$

$$\begin{bmatrix} u_{1sw}^* \\ u_{2sw}^* \end{bmatrix} = \begin{bmatrix} \frac{1}{\Gamma\alpha_m b^2 + I_B + R^2\alpha_M \tan^2(x_3)} & 0 \\ 0 & \frac{1}{\Gamma I_{wheels}} \end{bmatrix}^{-1} \left(\begin{bmatrix} \eta_{1\Delta}\,\mathrm{sgn}(s_1) \\ \eta_{2\Delta}\,\mathrm{sgn}(s_2) \end{bmatrix} \right) \tag{46}$$

SIMULATION STUDY

In this section the performance of the designed controller of sliding mode is compared with a linear controller in order to show the robustness of the controller in presence of disturbance and flowing fluid. It is shown that the SMC controller is more suitable for the present non-linear system since it is more robust and practical in real situations compared to linear controlling approaches. The main characteristics of the studied screw based in pipe robot in this paper and its related pipe specifications are mentioned in Table 1.

Feedback Linearization

As mentioned above the first step of designing a sliding mode controller is to linearize the system in an exact way. According to Eqs. (17,18) and based on the Table 1, the state space of the system is as:

$$\dot{X}=\begin{Bmatrix} x_2 \\ \dfrac{\dfrac{x_2}{100}-\left(2.9x_4(1+\tan(x_3))^2\right)+\dfrac{0.49\sin(x_3)\left(3+\dfrac{3x_2\sin(x_3)}{20}\right)}{1000}+\dfrac{0.168x_2x_4\sin(x_3)}{\cos^3(x_3)}+1.68}{\dfrac{0.084\sin^2(x_3)}{\sin^2(x_3)-1}-0.073}-\dfrac{1}{\dfrac{0.084\sin^2(x_3)}{\sin^2(x_3)-1}-0.073} \\ x_4 \\ \left(1.6x_2^2\left(0.168\tan(x_3)\left(1+\tan^2(x_3)\right)\right)-9.94x_2\left(1+\tan^2(x_3)\right)+3.3\right)\times10^8 \end{Bmatrix}+ \begin{bmatrix} \dfrac{1}{0.073-\dfrac{0.084\sin^2(x_3)}{\sin^2(x_3)-1}} & 0 \\ 0 & 3.33\times10^8 \end{bmatrix}\begin{bmatrix} T_m \\ T_s \end{bmatrix}+\begin{bmatrix} d(t) \\ 0 \end{bmatrix}; y=h(x)=\begin{bmatrix} x_1 \\ x_3 \end{bmatrix} \tag{47}$$

where in this paper, $d(t)=\sin(t)$ is considered as the disturbance exerted on the system. So according to Eq. (24) and considering, *r1=2* and *r2=2*, Eq. (24) can be rewritten as:

$$\begin{bmatrix} \ddot{y}_1 \\ \ddot{y}_2 \end{bmatrix}=\begin{bmatrix} \dfrac{\dfrac{x_2}{100}-\left(2.9x_4(1+\tan(x_3))^2\right)+\dfrac{0.49\sin(x_3)\left(3+\dfrac{3x_2\sin(x_3)}{20}\right)}{1000}+\dfrac{0.168x_2x_4\sin(x_3)}{\cos^3(x_3)}+1.68}{\dfrac{0.084\sin^2(x_3)}{\sin^2(x_3)-1}-0.073} \\ \left(1.6x_2^2\left(0.168\tan(x_3)\left(1+\tan^2(x_3)\right)\right)-9.94x_2\left(1+\tan^2(x_3)\right)\right)\times10^8 \end{bmatrix}+j(x)\begin{bmatrix} T_m \\ T_s \end{bmatrix} \tag{48}$$

where *j(x)* is:

$$j(x)=\begin{bmatrix} \dfrac{1}{0.073-\dfrac{0.084\sin^2(x_3)}{\sin^2(x_3)-1}} & 0 \\ 0 & 3.33\times10^8 \end{bmatrix}$$

So the control input based on feedback linearization can be computed as follow:

$$u=\begin{bmatrix} \dfrac{1}{0.073-\dfrac{0.084\sin^2(x_3)}{\sin^2(x_3)-1}} & 0 \\ 0 & 3.33\times10^8 \end{bmatrix}^{-1}\times \left(\begin{bmatrix} \dfrac{\dfrac{x_2}{100}-\left(2.9x_4(1+\tan(x_3))^2\right)+\dfrac{0.49\sin(x_3)\left(3+\dfrac{3x_2\sin(x_3)}{20}\right)}{1000}+\dfrac{0.168x_2x_4\sin(x_3)}{\cos^3(x_3)}+1.68}{\dfrac{0.084\sin^2(x_3)}{\sin^2(x_3)-1}-0.073} \\ \left(1.6x_2^2\left(0.168\tan(x_3)\left(1+\tan^2(x_3)\right)\right)-9.94x_2\left(1+\tan^2(x_3)\right)\right)\times10^8 \end{bmatrix}+\begin{bmatrix} v_1 \\ . \\ . \\ v_m \end{bmatrix}\right) \tag{49}$$

Table 1. The value of the physical parameters of the system

Symbol	Value	Definition	Unit
M	0.01	Wheel mass	Kg
M_h	1	Hull mass	Kg
M_m	1	Motor mass	Kg
R	0.02	Wheel radius	m
B	0.1	Leg length	m
A	0.014	Robot's Effective Cross Sectional Area	m^2
F_N	15	The normal force of passive spring	N
μ	0.2	Friction coefficient	-
I_B	10^{-4}	Hull polar Moment of Inertia	$Kg.m^2$
I_{WZ}, I_{WX}	10^{-8}	Wheel Moment of Inertia around the pipe axis	$Kg.m^2$
g	9.8	Gravity	$\frac{m}{s^2}$
Γ	3	Number of active wheels	-
I_{wheel}	$2*10^{-8}$	Wheel Moment of Inertia around the leg	$Kg.m^2$
C_D	0.5	Drag Coefficient	-
ρ	1	Fluid Density	$\frac{Kg}{m^3}$
V	3	Downward Velocity of the Fluid	$\frac{m}{s}$
K_f	0.01	Damping Constant	$N \cdot m \cdot s$
μ	0.2	Fluid Dynamic Viscosity	$\frac{Kg}{m \cdot s}$

Sliding Mode Control Design

In order to design the sliding mode controller, it is necessary to determine the errors and their related sliding surfaces. A parabolic movement versus time is considered as the desired path for both of states ($\emptyset$ *and* α) according to Eqs. (50,51):

$$x_{d1} = 0.35t^2 \tag{50}$$

$$x_{d3} = 0.1t^2 \tag{51}$$

So the errors can be stated as Eqs. (52,53).

$$\bar{e}_1 = \left[x_1 - 0.35t^2, \quad x_2 - 0.75t \right]^T \tag{52}$$

$$\bar{e}_2 = \left[x_3 - 0.1t^2, \quad x_4 - 0.2t \right]^T \tag{53}$$

Now it is possible to set the sliding surfaces. These surfaces are considered as a linear function of errors:

$$s_1 = c_1(x_1 - 0.35t^2) + c_2(x_2 - 0.75t) \tag{54}$$

$$s_2 = c_1'(x_3 - 0.1t^2) + c_2'(x_4 - 0.2t) \tag{55}$$

So according to Eqs. (35, 36) the derivative of sliding surfaces can be calculated as:

$$\dot{s}_1 = c_1\left(x_2 - 0.05\right) + \frac{\frac{x_2}{100} - \left(2.9x_4(1+\tan(x_3))^2\right) + \frac{0.49\sin(x_3)\left(3 + \frac{3x_2\sin(x_3)}{20}\right)}{1000} + \frac{0.168x_2x_4\sin(x_3)}{\cos^3(x_3)} + 1.68}{\frac{0.084\sin^2(x_3)}{\sin^2(x_3)-1} - 0.073} - \frac{1}{\frac{0.084\sin^2(x_3)}{\sin^2(x_3)-1} - 0.073}\begin{bmatrix} 0.35 \\ 0.1 \end{bmatrix} + d(t) \tag{56}$$

$$\dot{s}_2 = c_1'(x_4 - 0.005) + \left(1.6x_2^2\left(0.168\tan(x_3)\left(1+\tan^2(x_3)\right)\right) - 9.94x_2\left(1+\tan^2(x_3)\right) + 3.3\right)\times 10^8 \tag{57}$$

Thus, the control input results as follow:

$$\begin{bmatrix} u_1^* \\ u_2^* \end{bmatrix} = \begin{bmatrix} \dfrac{1}{0.073 - \dfrac{0.084\sin^2(x_3)}{\sin^2(x_3)-1}} & 0 \\ 0 & 3.33\times 10^8 \end{bmatrix}^{-1} \times$$
$$\left(-\begin{bmatrix} c_1(x_2 - 0.05) \\ c_1'(x_4 - 0.005) \end{bmatrix} - \right.$$
$$\begin{bmatrix} \dfrac{x_2}{100} - \left(2.9x_4(1+\tan(x_3))^2\right) + \dfrac{0.49\sin(x_3)\left(3+\dfrac{3x_2\sin(x_3)}{20}\right)}{1000} + \dfrac{0.168x_2x_4\sin(x_3)}{\cos^3(x_3)} + 1.68 & \dfrac{1}{\dfrac{0.084\sin^2(x_3)}{\sin^2(x_3)-1} - 0.073} \\ \left(1.6x_2^2\left(0.168\tan(x_3)\left(1+\tan^2(x_3)\right)\right) - 9.94x_2\left(1+\tan^2(x_3)\right) + 3.3\right)\times 10^8 & \end{bmatrix} \Bigg/ \frac{0.084\sin^2(x_3)}{\sin^2(x_3)-1} - 0.073 \Bigg] -$$
$$\left. \begin{bmatrix} \sin(t) \\ 0 \end{bmatrix} + \begin{bmatrix} 0.35 \\ 0.1 \end{bmatrix} - \begin{bmatrix} \eta_{1\Delta}\,\mathrm{sgn}(s_1) \\ \eta_{2\Delta}\,\mathrm{sgn}(s_2) \end{bmatrix} \right) \tag{58}$$

Kinematics and Dynamics Results

Based on the new designed screw in-pipe inspection robot and considering the inclined angle of its wheels, the path of the wheels forms a helical movement on the wall of the pipe. Consider the following trajectory as the desired path of the states ($\emptyset$ *and* α) based on Eqs. (50, 51), so in Figure 3 the path of the wheels related to the desired path of the mentioned states can be observed.

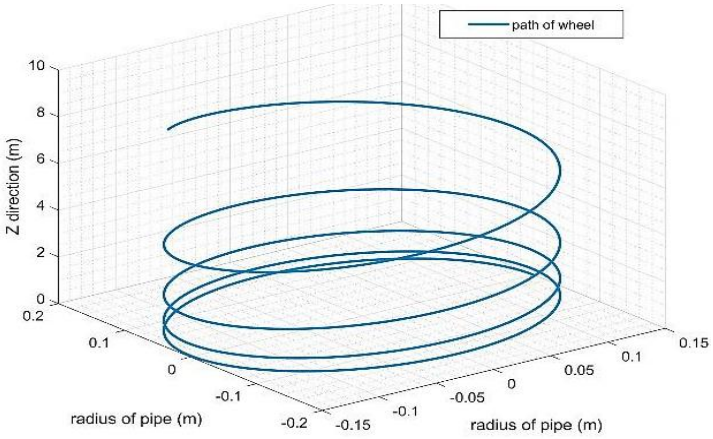

Figure 3. Path of wheels on the wall of pipe

Figure 3 shows the path of one wheel of the robot on the wall of the pipe. As mentioned, the new proposed in pipe robot in this paper is steerable and it is possible to change the pitch rate. So as figured above, it is noticeable that the pitch rate of the helical path is increasing as a results of changing the third state (α). Also the velocity of the center of the robots along the Z direction inside the pipe is illustrated in Figure 4.

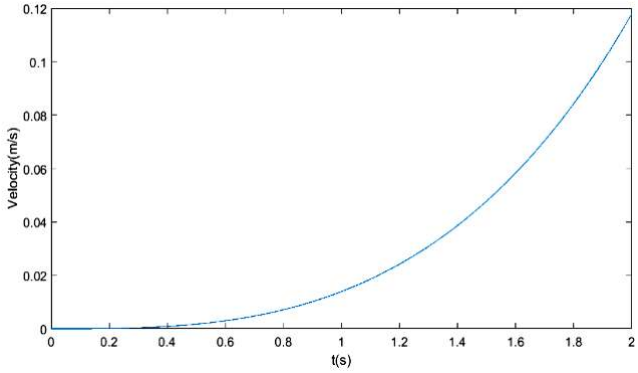

Figure 4. The Z direction velocity of the center of the robot through the pipe

As demonstrated in Figure 4, the velocity of the robot center through the pipe is increasing and the reason is contributed to the fact that the inclined angle of the wheels is enhancing. Finally considering the fact that the pipe which is modeled in this simulation is straight, the X and Y components of the velocity are zero and are not mentioned in the Figure 4. Joint space response relevant to the mentioned work space is also demonstrated in Figure 5.

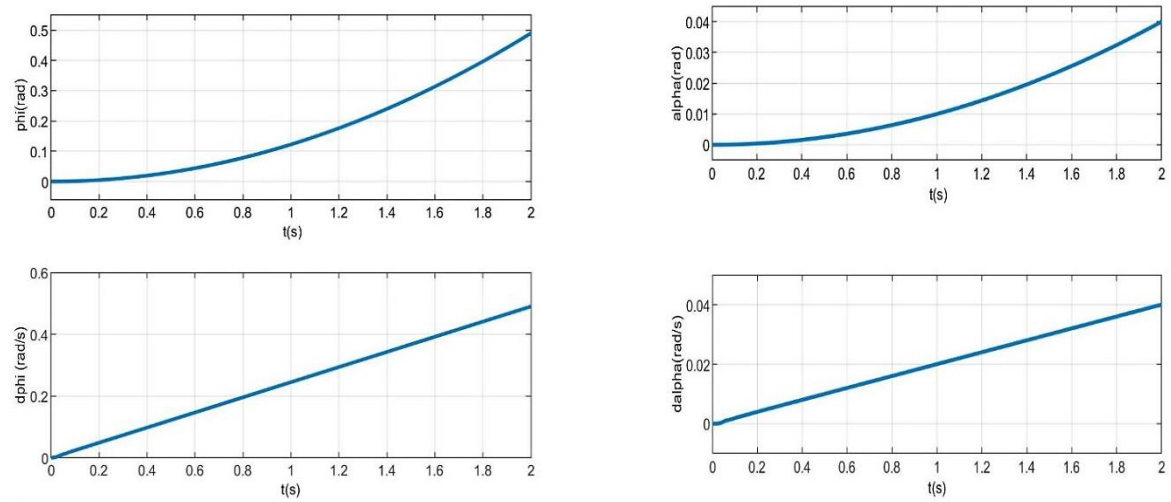

Figure 5. Responses of the joint space parameters

Considering the fact that the desire path of the position states ($\emptyset$ and α) are parabolic of order 2, it is expected that the velocity states ($\dot{\emptyset}$ and $\dot{\alpha}$) increase linearly. The kinetic inputs of the system based on the above joint space are shown in Figure 6. As shown in Figure 6 the inputs of the system in which no disturbance is implemented are calculate through the inverse dynamics of the system and as it can be seen are smooth.

Also the correctness of the modeling is verified in [32] by the same authors by comparing the results of MATLAB with the results of the modeled robot in ADAMS.

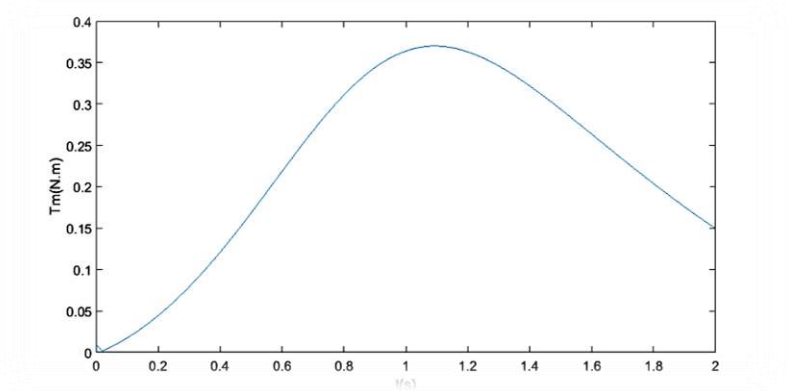

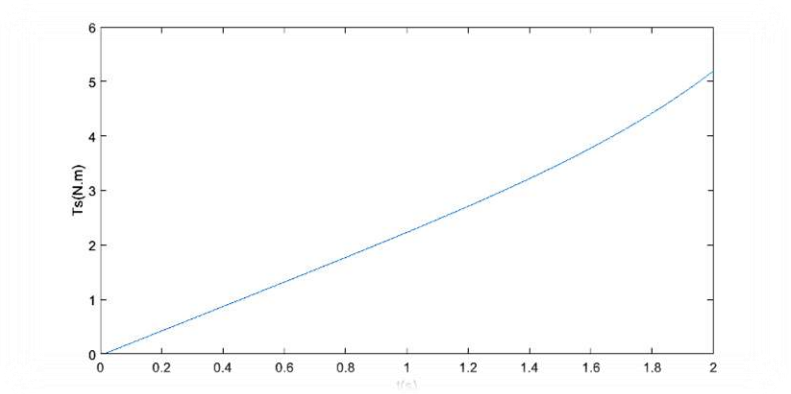

Figure 6. The inputs of system related to joint space

Control Results

To show the efficiency and robustness of the robot which is controlled using the proposed sliding mode controller respect to uncertainties and disturbances a comparison study is performed between SMC and LQR. Controlling parameters related to both controlling strategies of SMC and LQR are mentioned in Table 2. An external time dependent disturbance with the following function of Eq. (59) and a water stream with speed of 3 m/s is implemented on the robot in order to examine the robustness of the designed controller:

$$d(t) = \sin(t) \tag{59}$$

Table 2. The control parameters

Definition	Value
C_1 (the gain of first error)	*80*
C_1' (the gain of second error)	*30*
$\eta_{1\Delta}$ (the gain of sgn(s1))	*60*
$\eta_{2\Delta}$ (the gain of sgn(s2))	*20*
The controller gain (K_{LQR})	K_1 = *[2.2618 , 0.0180 , -10.6091 , 0.0063]* K_2 = *[3.0803 , 0.0184 , 0.7177 , 0.0887]*

In Figures 7 and 8, position states ($\emptyset$ *and* α) are compared between the mentioned controlling approaches to show the superiority of SMC in presence of disturbance and fluid flow.

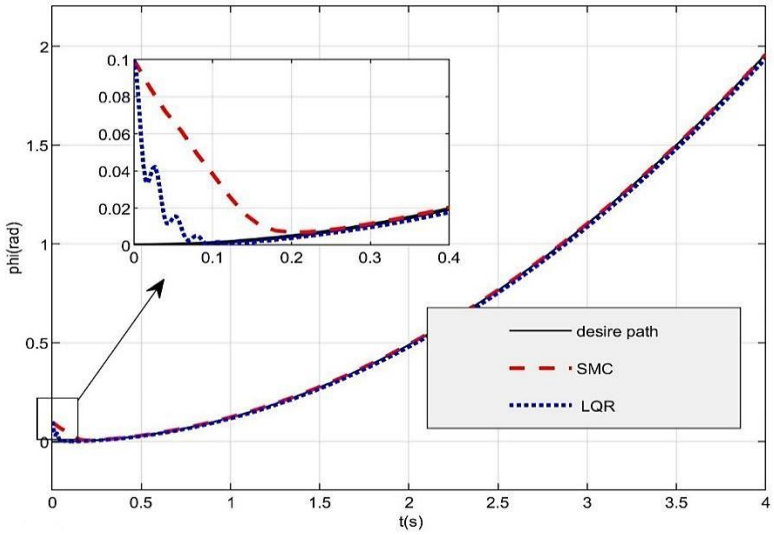

Figure 7. The comparison of the first state ($\emptyset$)

In Figure 7, it is shown that the SMC controller results in more smooth response in order to converge to the desire path compared to LQR specially at the initial moments of movement in which the response of LQR is under damped while the response of SMC is over damped. In addition, it can be seen in Figure 8 that the angle of the robot's wheels using LQR could not track the desired path accurately while again in SMC the response converges to its desired path in an over damped way. Thus it can be concluded that as it was expected SMC is more robust rather than a linear controller like LQR in presence of disturbances. The response of LQR not only has overshoot but also has a n error about 10% at its maximum stage. Although the first state (∅), related to LQR is acceptable, but again it will be shown that the requisite input for this response is not practical.

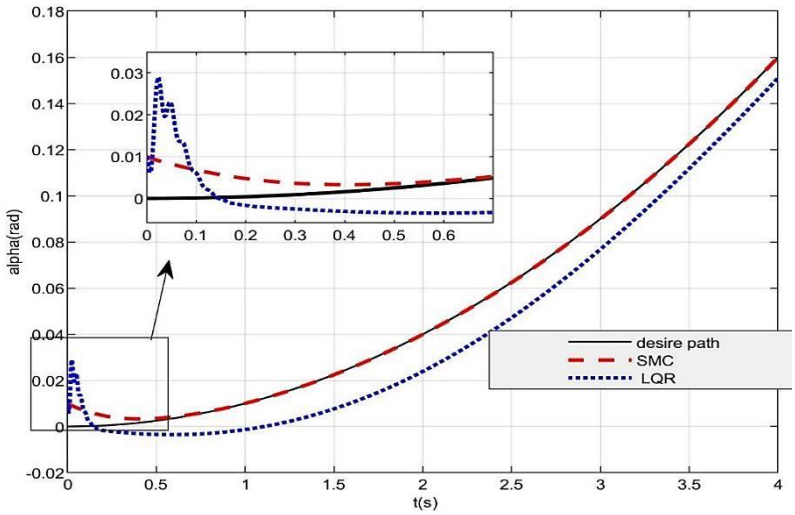

Figure 8. The comparison of the third state (α)

Control inputs of the system corresponding to the above response are depicted in Figure 9 and 10 in which, a comparison is performed again between the mentioned controlling approaches to show the optimality of SMC controller in presence of disturbance.

In Figure 9 and 10, it is remarkable that LQR approach requires big inputs to support the system to track the path and compensate the disturbance at the beginning which is near 10N.m for the first input and is 15N.m for the second input. But these amount of torques are too high which need strong motors and is not economical.

In contrast, SMC approach produces inputs near 2N.m that is optimum and more practical. It can be also observed that SMC provides higher input for the non-extremum intervals in order to neutralize the destructive effect of disturbances which is caused by fluid flow and so it can be concluded that the new designed non-linear controller based on SMC is more appropriate for the present system, especially in presence of disturbance and fluid stream. Also because of using the switching function of *tanh*, chattering phenomenon in inputs is decreased significantly.

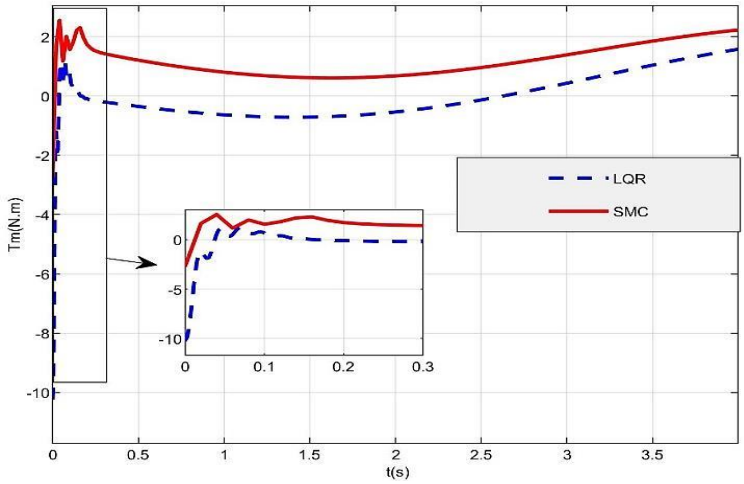

Figure 9. Comparison of the first input (T_m)

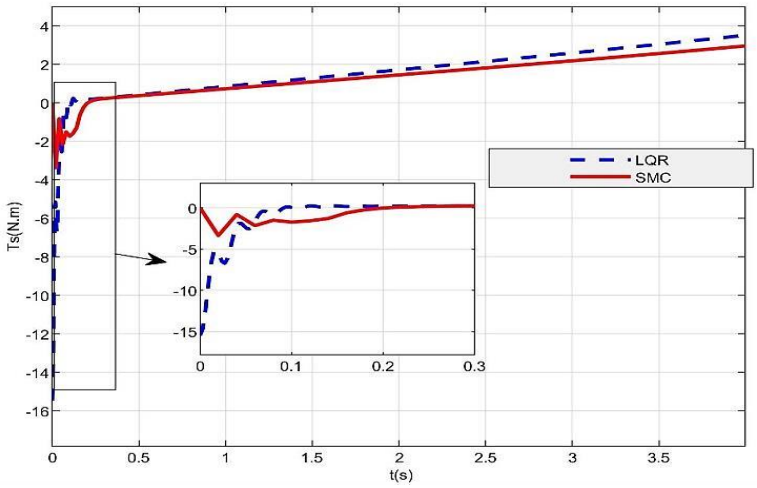

Figure 10. Comparison of the second input (Ts)

At the end, it is necessary to investigate the errors of the system for two cases to check the accuracy of the employed controllers. In Figures 11 and 12 the tracking errors of both controllers are shown.

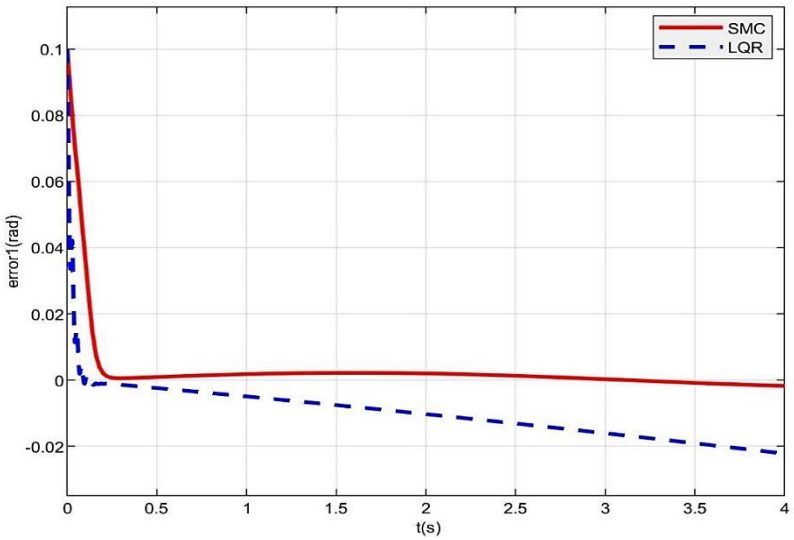

Figure 11. Error of the first state (φ)

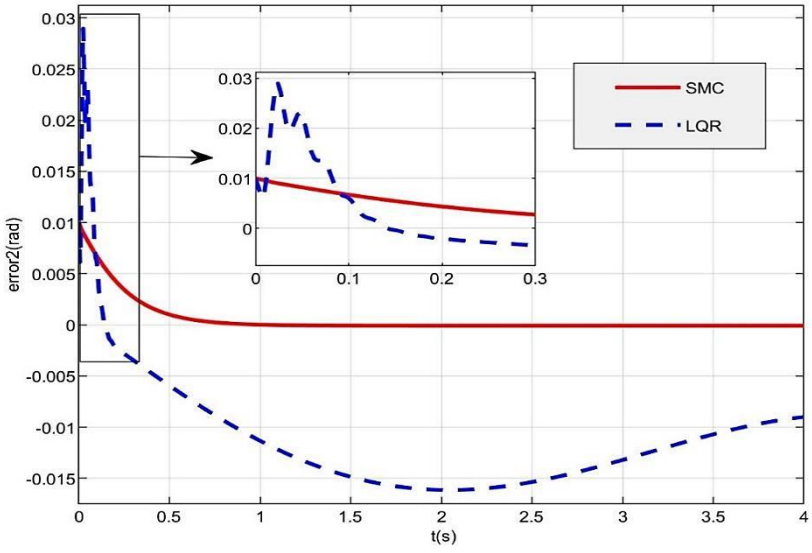

Figure 12. Error of the second state ($\boldsymbol{\alpha}$)

As seen above, the disturbance has a big influence on the responses of the system in the case in which the robot is controlled using LQR. On the other hand, as it was seen above, the error of the system in which it is controlled by the aid of SMC converges to zero in an over damped way which shows the superiority of this controller. Moreover, it should be noticed that since LQR is a linear controller and the in-pipe robot dynamic of the present paper is extremely nonlinear, domain of attraction of the system which is equipped by LQR is limited while SMC can be used for the whole workspace of the robot. So, Figures 13 and 14 show the domain of attraction of the position states.

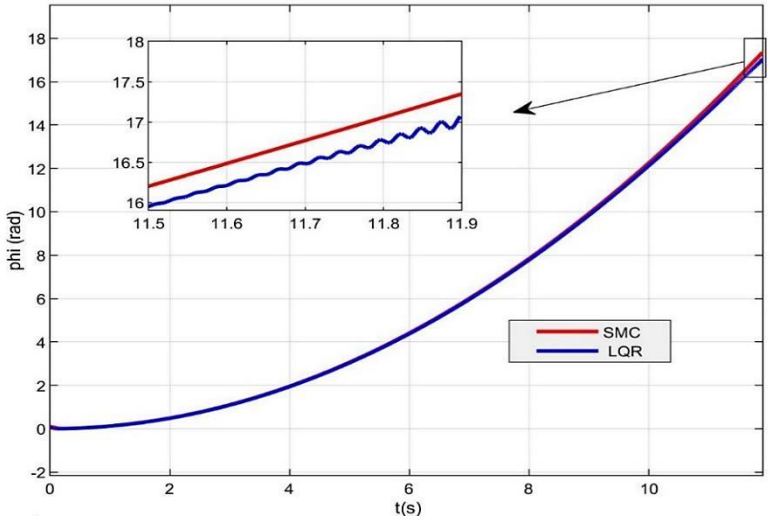

Figure 13. Domain of attraction of (φ)

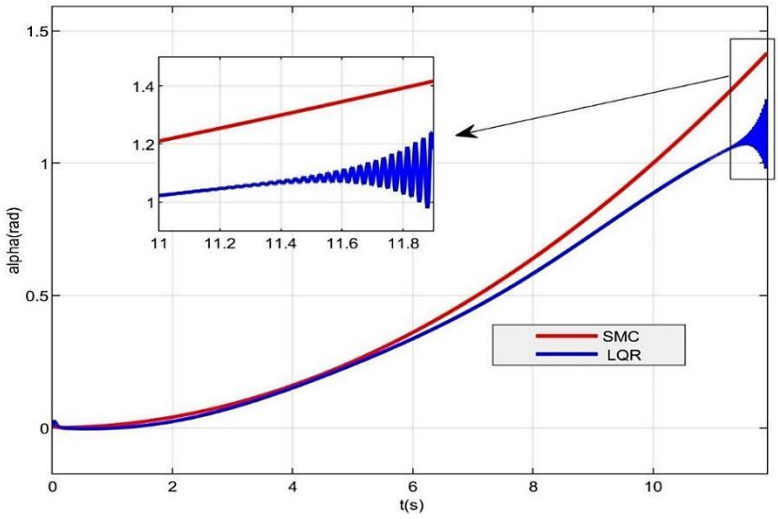

Figure 14. Domain of attraction of ($\boldsymbol{\alpha}$)

As demonstrated in Figures 13 and 14, SMC controller is working properly for the whole interval of the robot workspace while LQR controller becomes singular after entering in its singular zone. It is noticeable that, when LQR controller is going far from its operating point about which linearization is implemented, it becomes unstable and singular. Thus the domain of attraction related to the steering angle is about 1 rad while this domain is about 15 rad for the rotor angle. Therefore it can be concluded that the sensitivity of the rotor angle respect to the controller signal is less than the steering one.

Finally since the system is extremely impressible respect to the angle of the wheels, it is so significant to control the third state (α) with an acceptable accuracy which can be realized using SMC. In Figure 15 it is shown that the path of the wheels with LQR controller does not have an accurate response compared to the case in which the robot is controlled using SMC method. It can be seen that the error of LQR after 10sec is about 0.5meters. This huge error is the result of the error of the third state (α). So in this figure, it is proved that the influence of the inclined angle on the path of the wheels is efficiently important.

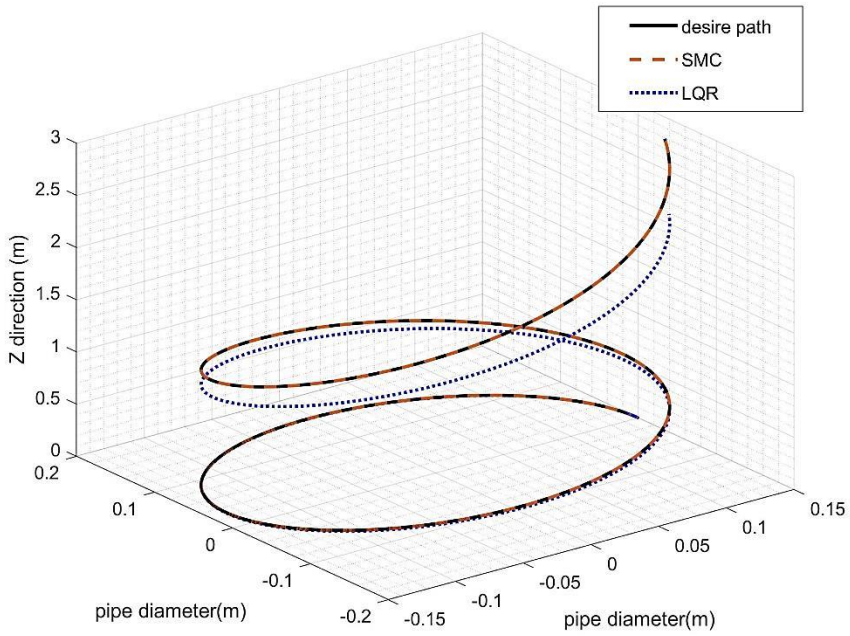

Figure 15. Path of the wheel in the pipe-wall

Finally, to show the influence of the fluid stream inside the pipe on the performance of the robot, there is a comparison between the first input of the system in Figure 16(b) between the robot which is exposed to the fluid stream and the robot which moves through an empty pipe. Both cases are controlled using the selected SMC controller and the response of the path and the first state are the same for both cases thanks to usage of the mentioned robust controller (Figure 16a).

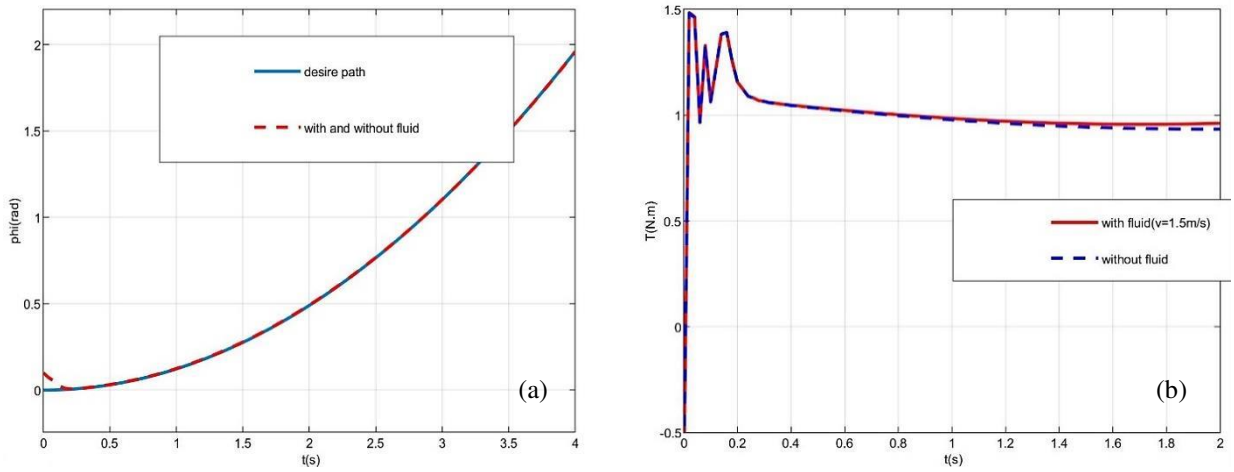

Figure 16. Comparison of the first input of the system

It is shown in Figure 16(b) when the robot is moving through an active pipe in which the flow of the fluid is not blocked the first input needs to be increased to maintain the robot in its stable situation. So not only the impact of fluid on system and its related modeling can be shown here but also the importance and necessity of design and implementation of a non-linear robust controller to ensure the stability of the robot can be highlighted.

MSC-ADAMS Verification

A verification is performed here in which the performance of the controlled robot is validated. To do so the plant of the system which is previously verified in [32] is modeled in ADAMS in presence of external disturbances and this plant is then exported to the SIMULINK. This modeled is controlled then by the aid of both the proposed SMC and conventional FL controllers. The performance of the system is compared for these two controllers in presence of drag force of fluid stream to show the efficiency of the proposed SMC control in presence of drag forces.

The inpipe inspection robot with the mentioned formulation of modeling section and kinematic and kinetic specifications of Table 3 is modeled in ADAMS as the plant of the system. The isometric view of the modeled robot in ADAMS is as Figure 17.

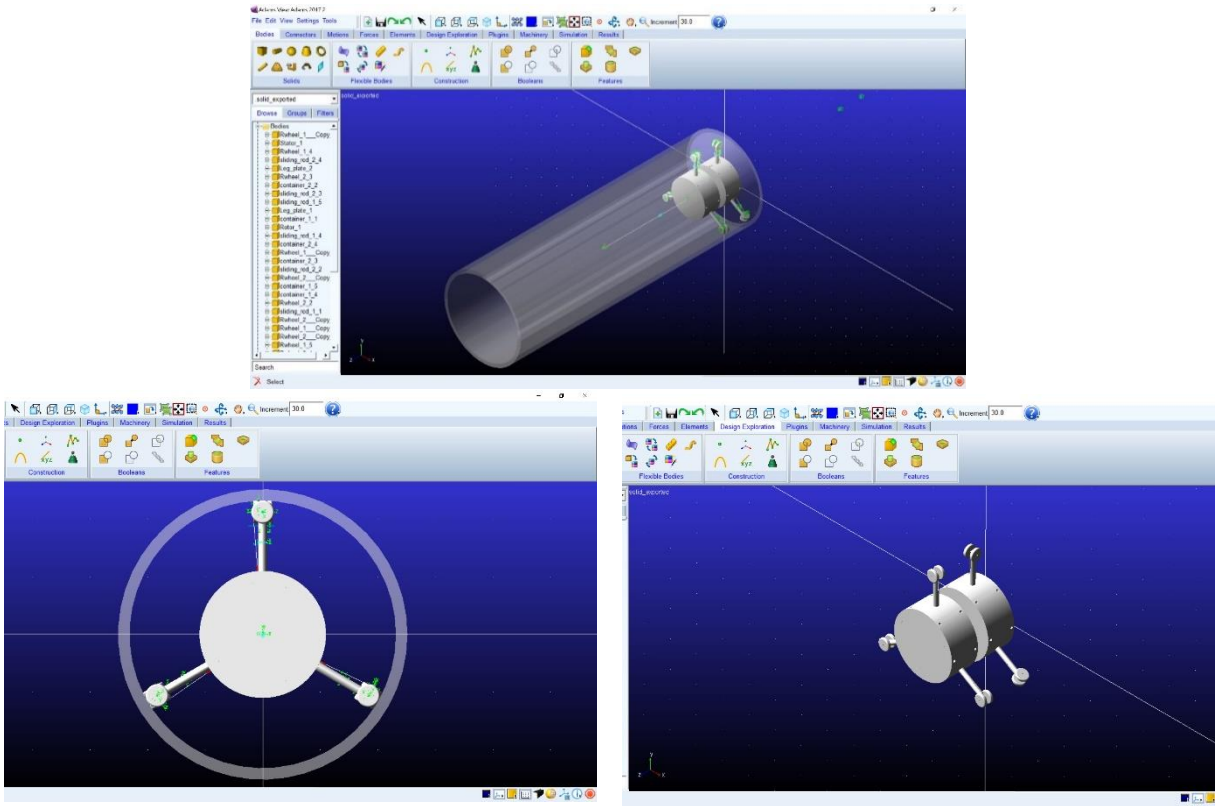

Figure 17. Modeled inpipe robot in ADAMS

Same kinematic and kinetic parameters of SIMULINK is employed for modeling the robot in ADAMS. The robot is modeled in the ADAMS with two separate parts of rotor and stator with the mentioned weights of Table 3. These two parts are finally assembled in ADAMS using a revolute joint. Within each part, three legged wheels are installed with relative degree of 120 degrees. The legs of the stator wheels are installed to their chassis using fixed constraint while the wheel legs of the rotor section is mounted on its corresponding chassis using a revolute joint in order to support the steering wheels. All of the three legs rotates simultaneously and equal employing a differential gear as their power transmission line. Whole the system is integrated by a cylindrical cover and the steering wheels are the robot locomotion mechanism which are driven by the rotor motor and the frictional force between the wheels and the pipe. In order to generate the required normal force of the wheels a suspension spring is considered between the chassis and the wheels and the corresponding spring coefficient is mentioned in the Table 3.

In order to check the efficiency of the proposed controller and compare it with a simple FL controller, the ADAMS model is exported to SIMULINK as the plant and two controlling strategies of FL and SMC are coded in SIMULINK as the controller of the system. The related Simulink circuit can be seen as Figure 18. To show the superiority of the proposed robust controller, a drag force of Eq. (60) is implemented to the plant and the performance of these two controllers are compared for tracking of Eq. (61):

$$d = AC_D\rho(Rx_2\tan(x_3)+v)^2 \tag{60}$$

$$\begin{aligned}\phi_d &= -0.1t^4 + 0.48t^3 - 0.25t^2 + 0.05t - 0.002\\ \alpha_d &= 0.06t^2 - 0.01t + 0.09\end{aligned} \tag{61}$$

Table 3. Modeling specification of the robot in ADAMS

Physical properties of the system			
Symbol	**Value**	**Definition**	**Unit**
M	0.012	Wheel mass	Kg
M_h	1.2	stator mass	Kg
M_m	1	Motor mass	Kg
R	0.01	Wheel radius	M
B	0.1	Leg length	M
A	0.014	Robot's Effective Cross Sectional Area	m^2
I_B	$0.3*10^{-4}$	Hull polar Moment of Inertia	$Kg.m^2$
Γ	3	Number of active wheels	-
C_D	1	Drag Coefficient	-
ρ	1	Fluid Density	$\frac{Kg}{m^3}$
V	4	Downward Velocity of the Fluid	$\frac{m}{s}$

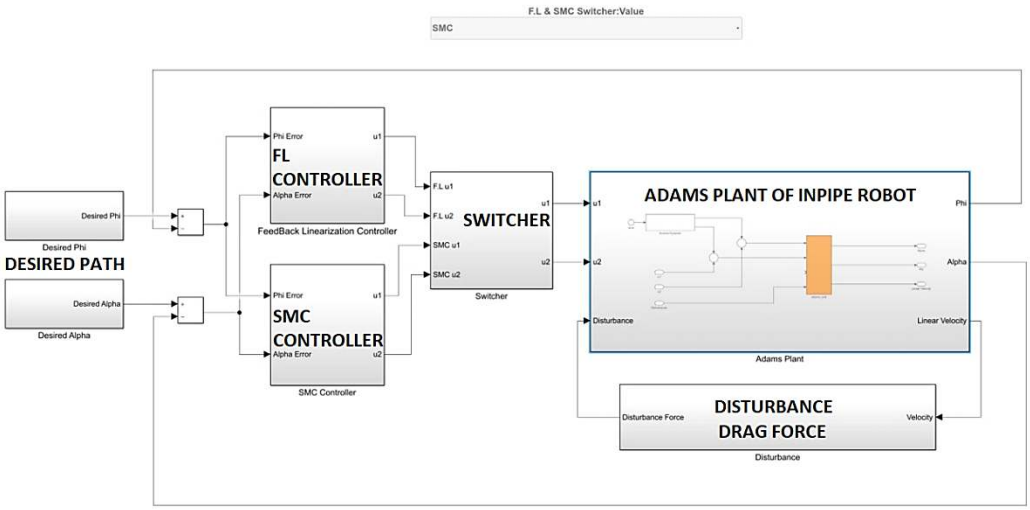

Figure 18. Control scheme of the ADAMS model in SIMULINK

The actual path of each controller and its comparison with the desired one is depicted in Figure 19. And its related error can be compared as Figure 20. As can be seen, the response accuracy of the plant which is controlled using SMC is significantly As can be seen, the response accuracy of the plant which is controlled using SMC is increased up to 90% with respect to FL and this is contributed to the fact that as mentioned the external drag force of the flowing fluid is a kind of external disturbance which should be neutralized using a robust controller like SMC. The error of this controller on the ADAMS plant is decreased about one tenth which shows that the proposed controller can practically control the inpipe robot of this paper in presence of pipe stream.

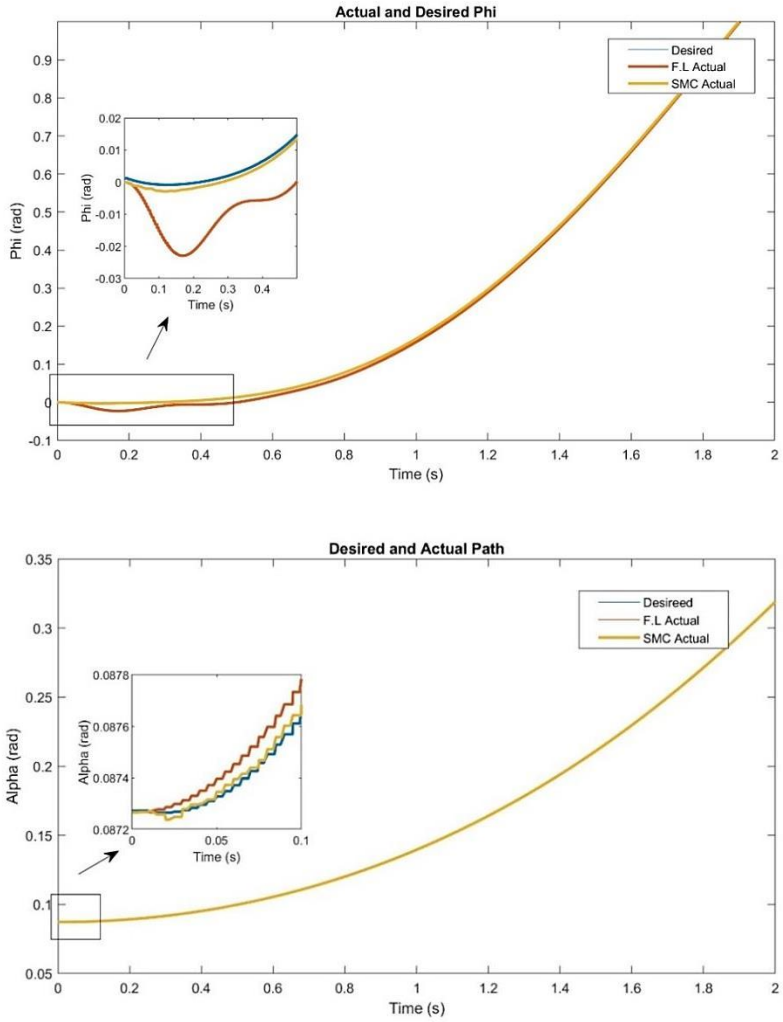

Figure 19. Desired path of the states and its comparison with the actual path for both controllers

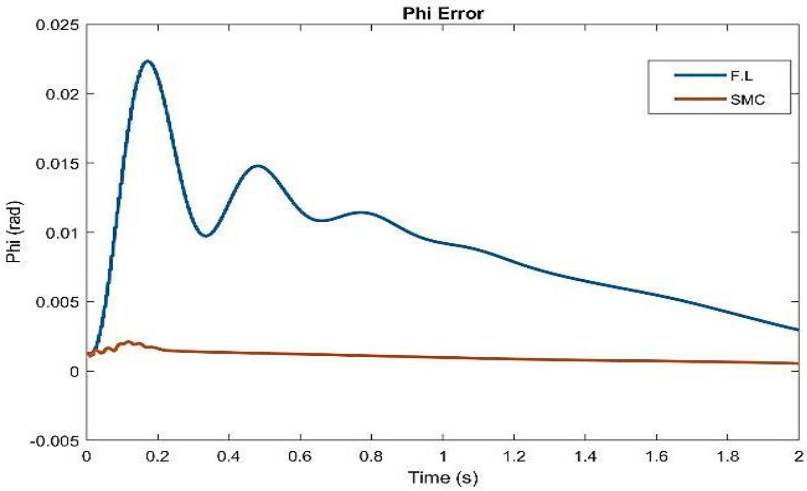

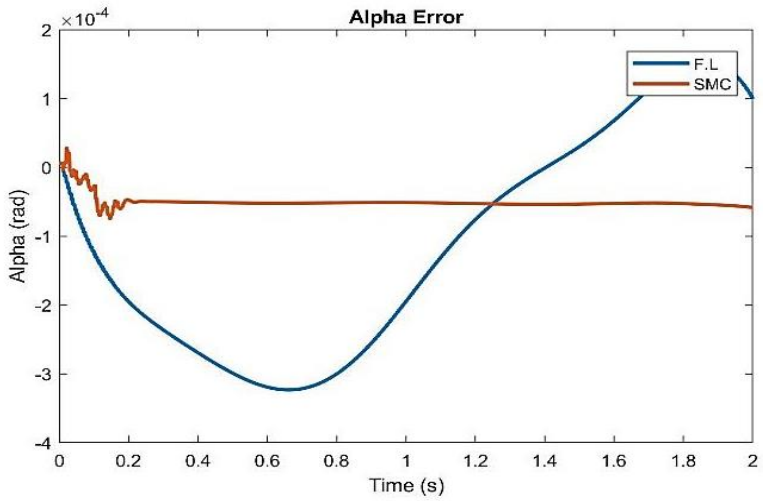

Figure 20. Comparison of error between FL and SMC

CONCLUSIONS

A modified version of screw based inpipe investigation robot was proposed in this paper equipped by a robust controller. Pitch rate of the robot is controllable as a result of its steerable wheels and thus the robot is able to bypass the obstacles. Also the robot was modeled in live pipes in presence of fluid flow and its motion was controlled by the aid of a robust controlling strategy i.e. SMC in presence of external disturbances of drag forces. Thus it was seen that using the proposed controlling strategy there is no need to block the pipe line flow. To meet this goal, kinematics and kinetics of the proposed in-pipe robot were completely represented. Afterwards, the nonlinear MIMO dynamics of the robot was linearized exactly and sliding mode control was employed to stabilize the robot in presence of external disturbing forces. In order to examine the performance of the proposed in-pipe robot and also applicability of the designed nonlinear controller, all of the mentioned modeling were simulated in MATLAB-SIMULINK. It was seen that the robot can track the desired path in presence of external disturbance of flowing fluid successfully with a good accuracy. The superiority of the designed robust and nonlinear controller of (SMC) was also shown with respect to LQR toward tracking the desired path in presence of disturbing drag force of flow. Moreover, it was seen that SMC provides the stability and accuracy of the system within the whole of the dynamic workspace of the robot while LQR has a limited domain of attraction. This improvement of SMC is the result of its higher consumption of energy to compensate the impact of the fluid. Finally, in order to verify the model and also prove the superiority of the proposed robust controller compared to conventional nonlinear controllers like FL the robot was modeled in ADAMS and its performance in presence of drag force was compared between SMS and FL. It was seen that the error of the system in which the SMC is employed is about one tenth of the latter case. Therefore, it can be concluded that the proposed designed non-linear controller of sliding mode control in this paper can successfully control the new nonlinear in-pipe inspection robot which has higher maneuverability in a robust way and in presence of disturbances and drag force of flowing fluid while the stability and accuracy of the system is also guaranteed.

REFERENCES

[1] KR. Simba, N. Uchiyama, and S. Sano, "Real-time smooth trajectory generation for nonholonomic mobile robots using Bézier curves," *Robotics and Computer-Integrated Manufacturing,* vol. 41, pp. 31-42, 2016.

[2] G. Scaglia, E. Serrano, A. Rosales, and P. Albertos," Linear interpolation based controller design for trajectory tracking under uncertainties: Application to mobile robots," *Control Engineering Practice*, vol. 45, pp. 123-132, 2015.

[3] V.F. Filaretov and V.E. Pryanichnikov, "Autonomous mobile university robots AMUR: Technology and applications to extreme robotics," *Procedia Engineering,* vol. 100, pp. 269-277, 2015.

[4] T. Liu and Z-P. Jiang, "Distributed formation control of nonholonomic mobile robots without global position measurements," *Automatica,* vol. 49, pp. 592-600, 2013.

[5] S. Jerban, and M.M. Moghaddam, "On the in-pipe inspection robots traversing through elbows," *International Journal of Robotics*, Theory and Applications. vol. 4, no. 2, pp. 19-27, 2015.

[6] K. Suzumori, S. Wakimoto, and M. Takata, "A miniature inspection robot negotiating pipes of widely varying diameter". In: *2003 IEEE International Conference on Robotics and Automation (Cat. No. 03CH37422)*: IEEE; 2003.

[7] K. Nagaya, T. Yoshino, M. Katayama, I. Murakami, and Y. Ando, "Wireless piping inspection vehicle using magnetic adsorption force," *IEEE/ASME Transactions on Mechatronics*, vol. 17, pp. 472-479, 2012.

[8] M. Ciszewski, T. Buratowski, M. Giergiel, P. Małka, and K. Kurc, "Virtual prototyping, design and analysis of an in-pipe inspection mobile robot," *Journal of Theoretical and Applied Mechanics*,vol. 52, pp. 417-429, 2014.

[9] Y-S. Kwon and B-J. Yi, "Design and motion planning of a two-module collaborative indoor pipeline inspection robot," *IEEE Transactions on Robotics*, vol. 28, pp. 681-696, 2012.

[10] J. Park, D. Hyun, W-H. Cho, T-H. Kim, and H-S. Yang, "Normal-force control for an in-pipe robot according to the inclination of pipelines," *IEEE transactions on Industrial Electronics*, vol. 58, pp. 5304-5310, 2010.

[11] Q. Liu, Y. Chen, T. Ren, and Y. Wei, "Optimized inchworm motion planning for a novel in-pipe robot," *Proceedings of the Institution of Mechanical Engineers, Part C: Journal of Mechanical Engineering Science*, vol. 228, pp. 1248-1258, 2014.

[12] E. Dertien, M.M. Foumashi, K. Pulles, and S. Stramigioli, "Design of a robot for in-pipe inspection using omnidirectional wheels and active stabilization," In: *2014 IEEE International Conference on Robotics and Automation (ICRA)*: IEEE; 2014.

[13] P. Li, S. Ma, C. Lyu, X. Jiang, and Y. Liu, "Energy-efficient control of a screw-drive pipe robot with consideration of actuator's characteristics," *Robotics and biomimetics,* vol. 3, pp. 1-11, 2016.

[14] A. Kakogawa, T. Nishimura, and S. Ma, "Designing arm length of a screw drive in-pipe robot for climbing vertically positioned bent pipes," *Robotica*, vol. 34, pp. 306-327, 2016.

[15] T. Li, S. Ma, B. Li, M. Wang, Z. Li, and Y. Wang, "Development of an in-pipe robot with differential screw angles for curved pipes and vertical straight pipes," *Journal of Mechanisms and Robotics,* vol. 9, 051014, 2017.

[16] P. Li, M. Tang, C. Lyu, M. Fang, X. Duan, and Y. Liu, "Design and analysis of a novel active screw-drive pipe robot," . *Advances in Mechanical Engineering*, vol. 10, 1687814018801384, 2018.

[17] Y. Chen, Q. Liu, T. Ren. "A simple and novel helical drive in-pipe robot". *Robotica* 2015, 33:920-932.

[18] G.H. Mills, J.H. Liu, B.Y. Kaddouh, A.E. Jackson, and R.C. Richardson, "Miniature magnetic robots for in-pipe locomotion," In: *Robotics Transforming the Future: Proceedings of CLAWAR 2018: The 21st International Conference on Climbing and Walking Robots and the Support Technologies for Mobile Machines*: CLAWAR Association Ltd; 2018.

[19] A. Nayak and S. Pradhan, "Design of a new in-pipe inspection robot," *Procedia Engineering,* vol. 97, pp. 2081-2091, 2014.

[20] H. Song, K. Ge, D Qu, H. Wu, and J. Yang, "Design of in-pipe robot based on inertial positioning and visual detection," *Advances in Mechanical Engineering*, vol. 8, no. 9, 1687814016667679, 2016.

[21] P. Li, S. Ma, B. Li, and Y. Wang, "Multifunctional mobile units with a same platform for in-pipe inspection robots," In: *2008 IEEE/RSJ International Conference on Intelligent Robots and Systems*: IEEE; 2008.

[22] Y. Zhang, M. Zhang, H. Sun, and Q. Jia, "Design and motion analysis of a flexible squirm pipe robot," In: *2010 International Conference on Intelligent System Design and Engineering Application*: IEEE; 2010.

[23] T. Li, S. Ma, B. Li, M. Wang, and Y. Wang, "Fuzzy theory based control method for an in-pipe robot to move in variable resistance environment," *Chinese Journal of Mechanical Engineering*, vol. 28, no. 6, pp. 1213-21, 2015.

[24] A.A. Pyrkin, A.A. Bobtsov, S.A. Kolyubin, M.V. Faronov, O.I. Borisov, V.S. Gromov, S.M. Vlasov, and N.A. Nikolaev, "Simple robust and adaptive tracking control for mobile robots," *IFAC-PapersOnLine*, vol. 48, pp. 143-149, 2015.

[25] A.H. Heidari, M. Mehrandezh, R. Paranjape, and H. Najjaran, "Dynamic analysis and human analogous control of a pipe crawling robot," In: *2009 IEEE/RSJ International Conference on Intelligent Robots and Systems*: IEEE; 2009.

[26] F. Inel, and S. Babesse, "Adaptive sliding mode control of a novel cable driven robot model". *Journal of Mechanical Engineering and Sciences*, vol. 13, no. 2, pp. 5150-62, 2019.

[27] K.D.H. Thi, M.C. Nguyen, H.T. Vo, V.M. Tran, D.D. Nguyen, and A.D. Bui, "Trajectory tracking control for four-wheeled omnidirectional mobile robot using backstepping technique aggregated with sliding mode control," In: *2019 First International Symposium on Instrumentation, Control, Artificial Intelligence, and Robotics (ICA-SYMP)*: IEEE; 2019.

[28] M.A. Shamseldin, M. Sallam, A.M. Bassiuny and A.A. Ghany, "Real-time implementation of an enhanced nonlinear PID controller based on harmony search for one-stage servomechanism system," J*ournal of Mechanical Engineering and Sciences*, vol. 12, no. 4, pp. 4161-4179, 2018.

[29] M.S. Rahmat, K. Hudha, Z. Abd Kadir, N.R.M. Nuri, N.H. Amer and S. Abdullah, "Modelling and control of a Magneto-Rheological elastomer for impact reduction," *Journal of Mechanical Engineering and Sciences*, vol. 13, no. 3, pp. 5259-5277, 2019.

[30] A. Kakogawa and S. Ma, "Mobility of an in-pipe robot with screw drive mechanism inside curved pipes," In: *2010 IEEE International Conference on Robotics and Biomimetics*: IEEE; 2010.

[31] A. Isidori, "Nonlinear control systems," *Springer Science & Business Media*, 2013.

[32] H. Tourajizadeh, M. Rezaei, and A. Sedigh, "Optimal control of screw in-pipe inspection robot with controllable pitch rate," *Journal of Intelligent & Robotic Systems*, vol. 90, pp. 269-286, 2018.